Faceting of Σ3 and Σ9 Grain Boundaries in Copper

B.B. Straumal[1], S.A. Polyakov[1,2], E. Bischoff[2], W. Gust[2], E.J. Mittemeijer[2]

[1]*Institute of Solid State Physics, Russian Academy of Sciences,*

Chernogolovka, Moscow District, 142432 Russia

[2]*Max-Planck-Institut für Metallforschung and Institut für Metallkunde,*

Seestr. 92, 70174 Stuttgart, Germany

Abstract. Faceting is a well documented phenomenon known both for surfaces and interfaces, particularly, grain boundaries (GBs). Faceting can be considered as a phase transition when the original surface or GB dissociates onto flat segments whose energy is less than that of the original surface or GB. For the investigation of GB faceting a cylindrical Cu bicrystal with an island grain was grown by the Bridgman technique. Grain *1* in this bicrystal is completely surrounded by grain *2*. The dissociation $\Sigma 9 \rightarrow \Sigma 3 + \Sigma 3$ proceeds during the growth of the bicrystal. The twins appear instead of $\{111\}_1/\{115\}_2$ or $(110)_{\Sigma 9 CSL}$ facet. GB faceting was studied at 1293 K, 1073 K, and 873 K The profiles of the GB thermal groove were analysed by atomic force microscopy. Wulff-Herring plots and GB phase diagrams have been constructed for the Σ3, Σ9 and Σ9+Σ3 GBs. With increasing temperature the facets with low-density CSL-planes disappear in the GB shape. GB roughening phase transition can be responsible for this phenomenon.

Keywords: grain boundaries, faceting, roughening, Cu, Σ3, Σ9, phase diagrams

1. Introduction

Faceting is a well documented phenomenon known both for surfaces and interfaces, particularly, grain boundaries (GBs) [1–4]. Faceting can be considered as a phase transition when the original surface or GB dissociates into flat segments whose energy is less than that of the original surface or GB. GB faceting proceeds only close to the so-called coincidence misorientations. In this case the lattices of both grains form the coincidence site lattice (CSL) characterized by the parameter Σ (reverse density of coincidence sites). In most cases the GB facets lie in the CSL planes with high density of coincidence sites. In [5] it has been shown that the GBs possess special structure and properties in limited areas of temperature T and misorientation θ close to a coincidence misorientation θ_Σ. In other words, by increasing $\Delta\theta = |\theta - \theta_\Sigma|$ and T the phase transition "special GB – general GB" proceeds and the GB looses its special structure and properties [6]. The higher Σ, the lower the temperature and Δθ at which a GB losses its special structure and properties. This is due to the fact that for the CSLs with low Σ the depth of the energetic profile for the dense packed CSL planes is higher than that of high-Σ CSLs. Therefore, due to the temperature disordering the energetically favourable GB positions disappear at lower T for GBs with higher Σ [7]. Similar phenomena can be expected also for GB facets lying in different CSL planes. We can expect that at high temperature only the facets with highest density of coincidence sites appear, and with decreasing temperature the number of existing facets will gradually increase, including the facets with less and less dense packed coincidence sites and shallower energetic minima. The best objects for the search of this phenomenon would be the CSLs where

the different CSL planes do not have very different density of coincidence sites. CSL with $\Sigma = 9$ fulfils this condition [8, 9]. In fact, the results of computer modelling for CSL with $\Sigma = 9$ show that the GB lying along different CSL planes possess very similar energy [9].

2. Experimental

For the investigation of GB faceting, a cylindrical Cu bicrystal with an island grain was grown by the of Bridgman technique from Cu of 99.999 wt. % purity. The grain *1* in this bicrystal is completely surrounded by the grain *2* forming the Σ9 <110>tilt GB. The <110> axes in both grains are parallel to the growth axis. Therefore, the Σ9 <110> tilt GB in the sample contains all crystallographically possible inclinations. 2.5 mm thick platelets were cut from the grown bycrystal perpendicularly to the growth axis. The platelets were ground with 4000 SiC paper and polished with 3 and 1 μm diamond paste. After that they were annealed in 80% Ar + 20% H_2 gas mixture at pressure of 2×10^4 Pa at different temperatures (1293 K, 48 h; 1073 K, 2374 h and 873 K, 2391 h). The annealed samples were than etched in the 50% HNO_3 aqueous solution. The GB shape and geometry of facets were analysed and photographed in polarized light in bright and dark field with the aid of an Zeiss Axiophot optical microscope. The sample annealed at 1293 K was then carefully repolished and annealed 48 h once again in order to form GB thermal grooves. The profiles of the formed GB thermal groove were analysed with the aid of a Topometrix 2000 Explorer atomic force microscope (AFM) operating in the contact mode. The typical field analyzed with the aid of AFM had a dimension 50×50 μm containing 500×500 pixels. For the analysis, each 10

neighbouring profiles were used to obtain a mean profile. The ratio between GB energy σ_{GB} and surface energy σ_{sur} was calculated using the values of measured GB groove angles.

3. Results and discussion

It is well documented in the literature that close to the {111}/{115} inclination the Σ9 GB is unstable against the dissociation reaction: $\Sigma 9 \rightarrow \Sigma 3 + \Sigma 3$. This dissociation proceeds also in our case. The twins appear during the growth of bicrystal instead of $\{111\}_1/\{115\}_2$ or $(110)_{\Sigma 9CSL}$ facets (the subscripts 1 and 2 correspond to the grains *1* and *2*). The Σ3 twins were not present in the seeds. This fact permitted us to study the faceting of both Σ3 and Σ9 GBs simultaneously in the same samples.

In Table 1 the data on the Σ3 facets present in our samples after annealing at 1293, 1073 and 873 K are collected together with the data available in the literature. The twin plates after annealings at 1293, 1073 and 873 K are shown in Fig. 1. The energy of symmetric Σ3 twin ($\{111\}_1/\{111\}_2$ or $(100)_{\Sigma 3CSL}$ facet) is very low. The second close packed plane is $\{211\}_1/\{211\}_2$ or $(010)_{\Sigma 3CSL}$ facet, the so-called asymmetric twin. The angle between facets $(100)_{\Sigma 3CSL}$ and $(010)_{\Sigma 3CSL}$ is 90°. The presence of such facets are well documented for Al, Au, $AuCu_3$, and Ge [18–21]. The typical rectangular twin plates with $(100)_{\Sigma 3CSL}$ and $(010)_{\Sigma 3CSL}$ facets can be seen, for example in Au thin films [19]. However, the twin plates in Cu and Ag are not rectangular. The end facet forms an angle of 82° with the $\{111\}_1/\{111\}_2$ or $(100)_{\Sigma 3CSL}$ sides [11, 22]. TEM studies

revealed that this 82° facet has so-called 9*R* structure forming a plate of bcc GB phase in the fcc matrix [10, 23, 24]. Such $(100)_{\Sigma 3CSL}$ and 82° 9*R* facets on the Σ3 twin plate are clearly seen also in our samples in Fig. 1a (1293 K) and 1b (1073 K). Moreover, analysis of the literature shows that the 82° 9*R* facet appears in Cu only at high temperatures. At low temperatures the "normal" 90° $(010)_{\Sigma 3CSL}$ facets are present also in Cu (see Table 1). Therefore, the GB phase transition seems to occur close to 0.64 T_m. (T_m being the melting temperature). The $\{211\}_1/\{211\}_2$ or $(010)_{\Sigma 3CSL}$ facet has to disappear with increasing temperature. The 82° 9*R* facet appears instead of the 90° $(010)_{\Sigma 3CSL}$ facet. In our samples annealed at 873 K the 90° $(110)_{\Sigma 3CSL}$ facet appears at an angle of 55° to the symmetric twin facets $(100)_{\Sigma 3CSL}$ (Fig. 1c). To the best of our knowledge, the $(110)_{\Sigma 3CSL}$ facets were never observed before. Therefore, the GB phase transition seems to occur between 0.64 and 0.79 T_m. In Fig. 2 the phase diagram for Σ3 GBs is presented in coordinates "temperature T/T_m – inclination angle θ". Such phase diagrams are commonly used for the description of phase transitions on the free surfaces of crystals [2–4]. Some minor $(210)_{\Sigma 3CSL}$ and $(130)_{\Sigma 3CSL}$ facets are also present in the samples at 1293 and 1073 K. The length of these facets is only about few per cent of overall length of Σ3 GBs. To the best of our knowledge, such Σ3 facets in Cu were also never reported in the literature. In Fig. 3 the Wulff-Herring plot is shown for the Σ3 GBs at 1293 K constructed using the σ_{GB}/σ_{sur} ratios measured with the aid of AFM. The very low energy of coherent $(100)_{\Sigma 3CSL}$ facets determine the platelet-like form of twins in Cu. The metastable nature of the minor $(210)_{\Sigma 3CSL}$ and $(130)_{\Sigma 3CSL}$ facets is clearly seen. The presence of the flat $(210)_{\Sigma 3CSL}$ and $(130)_{\Sigma 3CSL}$ facets in the sample reveal the existence of the energetic minima on the Wulff-Herring plot. However, it

follows from Fig. 3, that these minima are not deep enough to allow the corresponding facets to be stable. In Fig. 4 the scheme of the Wulff-Herring plot is shown for 873 K. A deep energetic minimum exists at the $(110)_{\Sigma 3CSL}$ inclination and the $(110)_{\Sigma 3CSL}$ facet appears in the equlibrium shape (Fig. 1c).

In Table 2 the data are collected on the Σ9 facets present in our samples after annealing at 1293, 1073 and 873 K together with the data available in the literature. In Fig. 5 the corresponding phase diagram for Σ9 GBs is presented in co-ordinates "temperature T/T_m – inclination angle θ". As mentioned above, the $(110)_{\Sigma 9CSL}$ facet is unstable against the dissociation into two Σ3 GBs. Therefore, the point with doubled $(100)_{\Sigma 3CSL}$ energy appears at the Σ9 Wulff-Herring plot instead of the energy of the $(110)_{\Sigma 9CSL}$ facet (Fig. 5). At 1293 K only two facets are present in the sample, namely $(-1,1,0)_{\Sigma 9CSL}$ and $(-1,2,0)_{\Sigma 9CSL}$. This fact is reflected by the shape of the Wulff-Herring plot (Fig. 6). At lower temperatures additional facets appear (see Table 2 and Fig. 5) like $(100)_{\Sigma 9CSL}$, $(010)_{\Sigma 9CSL}$ and $(-1,2,0)_{\Sigma 9CSL}$. At 873 K the $(-1,3,0)_{\Sigma 9CSL}$ facet appears instead of the $(-1,2,0)_{\Sigma 9CSL}$ facet.

The possible faceting-defaceting and roughening GB phase transitions were recently discussed [1]. The first direct and deliberate observations of the reversible defaceting transition were made by Hsieh and Balluffi for asymmetric tilt GBs in Al and Au [25]. Westmacott and Dahmen observed that a small Al grain embedded in another Al grain had a polyhedral shape at low temperatures [26]. At high temperature the flat symmetric GB segments became rounded indicating a roughening transition. In our observations

the $(100)_{\Sigma 3CSL}$ and 9*R* facets always have sharp edges at their intersections. In contrast, the intersections of minor $(210)_{\Sigma 3CSL}$ and $(130)_{\Sigma 3CSL}$ facets with 9R facets are always rounded. The intersections of all Σ9 facets are clearly rounded. Generally, all facet intersections become less and less rounded with decreasing temperature. This can be the indication of a roughening-faceting phase transition. These transitions were predicted originally by Burton et al. for singular free surfaces [27]. The planar surface becomes curved with increasing temperature when the thermal energy becomes comparable with depth of energetic minimum for the planar surface [28]. In our case the GB facets positioned in less densely packed CSL planes (e.g. with shallower energetic minima) become planar with decreasing temperature. The GB roughening seems to be a reasonable expalanation for this phenomenon. The change of the shape of intersections of the GB facets and their energy in dependence on the temperature has to be carefully studied in the future.

Acknowledgements

The fruitful discussions with Prof. E. Rabkin, Prof. H.-E. Schaefer and Dr. L. Klinger are heartily acknowledged. This work was supported by the Russian Foundation of Basic Research (RFBR) under contract 01-02-16473, INTAS Programme under contract 99-1216, Deutsche Forschungsgemeinschaft under contracts Gu 258/12-1 and Gu 258/18-1, German Federal Ministry for Education and Research (BMBF) under WTZ-Project RUS 00/209 and exchange programme between Russian Academy of Sciences and Israel Science Foundation founded by the Academy of Sciences and Humanities. On of us (SAP) expresses his gratitude to the Max-Planck-Institut für Metallforschung

for the financial support of his research atay in Stuttgart. BBS would like to thank RFBR for the travel grant for the participation at iib-2001.

References

1. S. B. Lee, D. Y. Yoon, and M. F. Henry, Acta mater. 48, 3071 (2000).
2. M. Yoon, S. G. J. Mochrie, M. V. Tate, S. M. Gruner, E. F. Eikenberry, Surf. Sci. 411, 70 (1998).
3. G. M. Watson, D. Gibbs, S. Song, A. R. Sandy, S. G. J. Mochrie, D. M. Zener, Phys. Rev. B 52, 12329 (1995).
4. S. Song, S. G. J. Mochrie, Phys. Rev. B 51, 10068 (1995).
5. B. B. Straumal, and L. S. Shvindlerman, Acta metall. 33, 1735 (1985).
6. E. L. Maksimova, L. S. Shvindlerman, and B.B. Straumal, Acta metall. 36, 1573 (1988).
7. A. A. Zisman, and V. V. Rybin, Poverkhnost', No. 7, 87 (1982) in Russian.
8. G. D. Sukhomlin, and A. V. Andreeva, phys. stat. sol. (a) **78**, 333 (1983).
9. K. L. Merkle, and D. Wolf, Phil. Mag. A **65**, 523 (1992).
10. U. Wolf, F. Ernst, T. Muschik, M.W. Finnis, and H.F. Fischmeister, Phil. Mag. A 66, 991 (1992).
11. T. Muschik, W. Laub, M. W. Finnis, and W. Gust, Z. Metallk. **84**, 596 (1993).
12. T. Muschik, W. Laub, U. Wolf, M. W. Finnis, and W. Gust, Acta metall. mater. **41**, 2163 (1993).
13. W. Laub, A. Oswald, T. Muschik, W. Gust, and R.A. Fournelle in Solid–Solid Phase Transformations, edited by W.C. Johnson et al. (The Minerals, Metals & Materials Society, Warrendale, PA, 1994) p. 1115.

14. A. Oswald, W. Laub, W. Gust, and R.A. Fournelle, in Solid–Solid Phase Transformations, edited by W.C. Johnson et al. (The Minerals, Metals & Materials Society, Warrendale, PA, 1994) p. 1121.
15. F. Ernst, M. W. Finnis, A. Koch, C. Schmidt, B. Straumal, and W. Gust, Z. Metallk. **87**, 911 (1996).
16. C. T. Forwood, and L. M. Clarebrough, Acta metall. **32**, 757 (1984).
17. L. M. Clarebrough, and C. T. Forwood, phys. stat. sol. (a) **60**, 51 (1980).
18. J. M. Pénisson, U. Dahmen, and M. J. Mills, Phil. Mag. Lett. 64, 277 (1991).
19. P. J. Goodhew, T. Y. Tan, and R. W. Balluffi, Acta metall. 26, 557 (1978).
20. F. D. Tichelaar, and F. W. Schapink, J. Phys. Paris, C5, 49, 293 (1988).
21. A. Bourret, and J. J. Bacmann, Inst. Phys. Conf. Series 78, 337 (1985).
22. A. Barg, E. Rabkin, and W. Gust, Acta metall. mater. 43, 4067 (1995).
23. F. Ernst, M.W. Finnis, D. Hoffmann, T. Muschik, U. Schönberger, and U. Wolf, Phys. Rev. Lett. **69**, 620 (1992).
24. D. Hofmann, M. W. Finnis, Acta metall. mater. 42, 3555 (1994).
25. T. E. Hsieh, and R. W. Balluffi, Acta metall. 37, 2133 (1989).
26. K. H. Wetmacott, and U. Dahmen, in Interface: Structure and Properties, edited by S. Ranganathan, C. S. Pande, B. B. Rath and D. A. Smith (Trans Tech Publications, Uetikon-Zuerich, 1993), p. 133.
27. W. K. Burton, N. Cabrera, and F. C. Frank, Philos. Trans. A 243, 299 (1951).
28. C. Jayaprakash, W. F. Saam, and S. Teiltel, Phys. Rev. Lett. 50, 2017 (1983).

Table 1. The presence of different Σ3 facets at different temperatures in Cu. Corresponding inclination angles θ for various CSL planes are also given. Minory facets are marked as (m).

Facet	(100)	(010)	9*R*	(110)	(210)	(130)	Reference
θ, deg	0	90	82	55	71	25	
T/T_m							
0.95	+	-	+	-	+(m)	+(m)	This work
0.87	+	-	+	-			[10–14]
0.87	+	-	+	-			[10, 15]
0.79	+	-	+	-	-	+(m)	This work
0.64	+	-	+	+			This work
0.64	+	+	-	-			[16]
0.36	+	+	-	-			[17]
0	+	+	-	-			[9]

Table 2. The presence of different Σ9 facets at different temperatures in Cu. Corresponding inclination angles θ and density of coincidence sites S/S_{min} for various CSL planes are also given. Dissociated facets are marked as *Diss.*

Facet	(110)	(-110)	(100)	(010)	(310)	(-130)	(210)	(510)	(-120)	Refer.
θ, deg	0	71	126	35	152	131	162	142	55	
S/S_{min}	1	1	1.16	1.63	1.98	2.52	2.83	3.00	3.464	[8]
T/T_m										
0.95	Diss.	+							+	This work
0.79	Diss.	+	+	+					+	-"-
0.64	Diss.	+	+	+		+			Diss.	-"-
0.68	Diss.		+	+	+	+	+	+	+	[8]
0.64	+			+				+		[16]
0	Diss.		+	+	+				+	[9]

(a)
(b)
(c)

Fig. 1. Light micrographs showing the shape of Σ3 twin plates at (a) 1293, (b) 1073 and (c) 873 K. (a, b) Twin plates contain (100) $_{\Sigma 3CSL}$ and 82° 9*R* facets. (c) Twin plates contain (100) $_{\Sigma 3CSL}$, 82° 9*R* and 55° (110) $_{\Sigma 3CSL}$ facets.

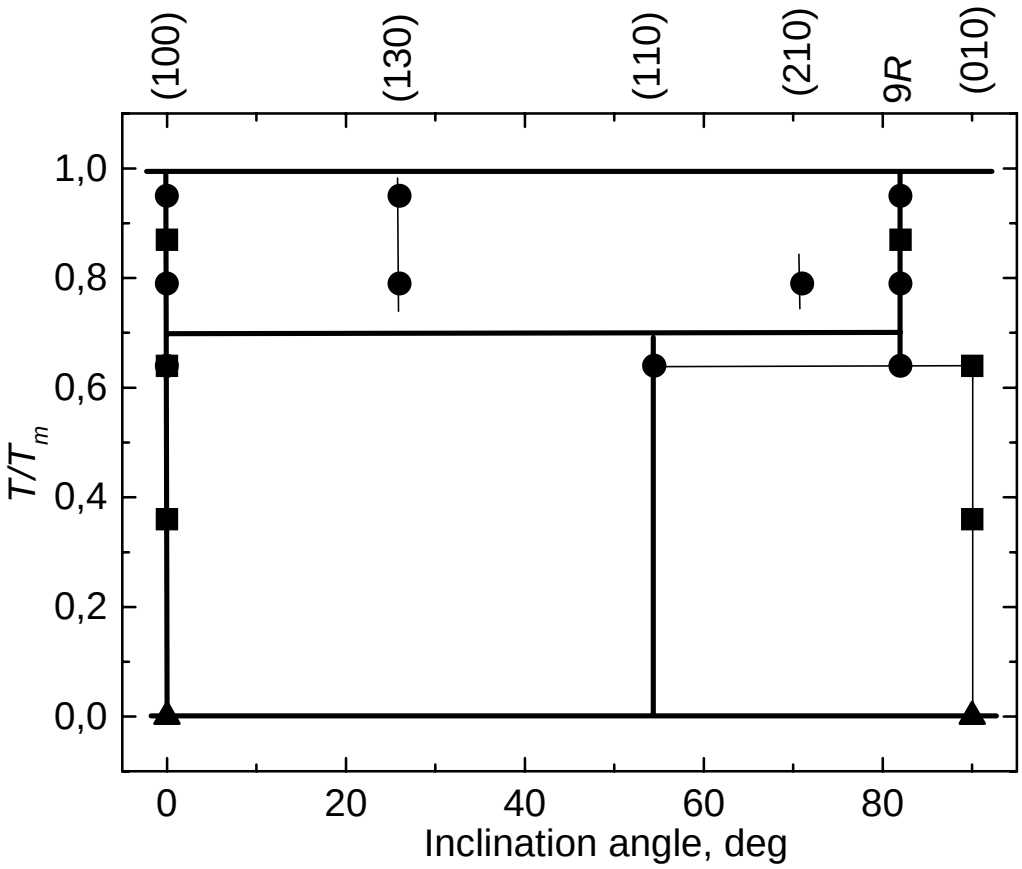

Fig. 2. Phase diagram for the various Σ3 facets. T_m is the melting temperature. The inclinations of Σ3 CSL planes are shown at the top of the diagram. Circles denote the facets experimentally observed in this work at 0.95 T_m (1293 K), 0.79 T_m (1073 K) and 0.64 T_m (873 K). Squares denote the facets experimentally observed at 0.87 T_m [10–15, 23], at 0.64 T_m [16] and at 0.36 T_m [17]. Triangles denote the energetic minima obtained using computer modelling [19]. Thick lines denote the temperature ranges of the stability for the major GB facets obtained in this work. Thin lines denote the (1) minor facets $(120)_{CSL}$ and $(210)_{CSL}$ observed in this work and (2) the range of existence for the $(010)_{CSL}$ facet and low-temperature boundary for the 9*R* facet based on the comparison of our data with published observations of other authors [16, 17]. Horizontal lines denote the upper limits of stability for $(110)_{CSL}$ and $(010)_{CSL}$ facets.

The figure may be reduced to the one-column size

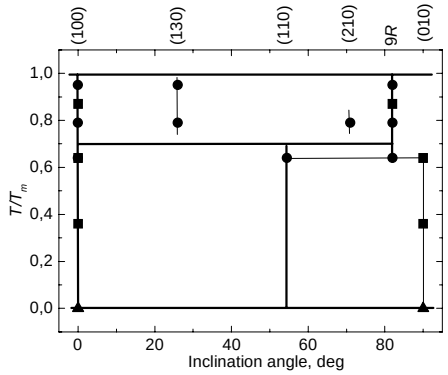

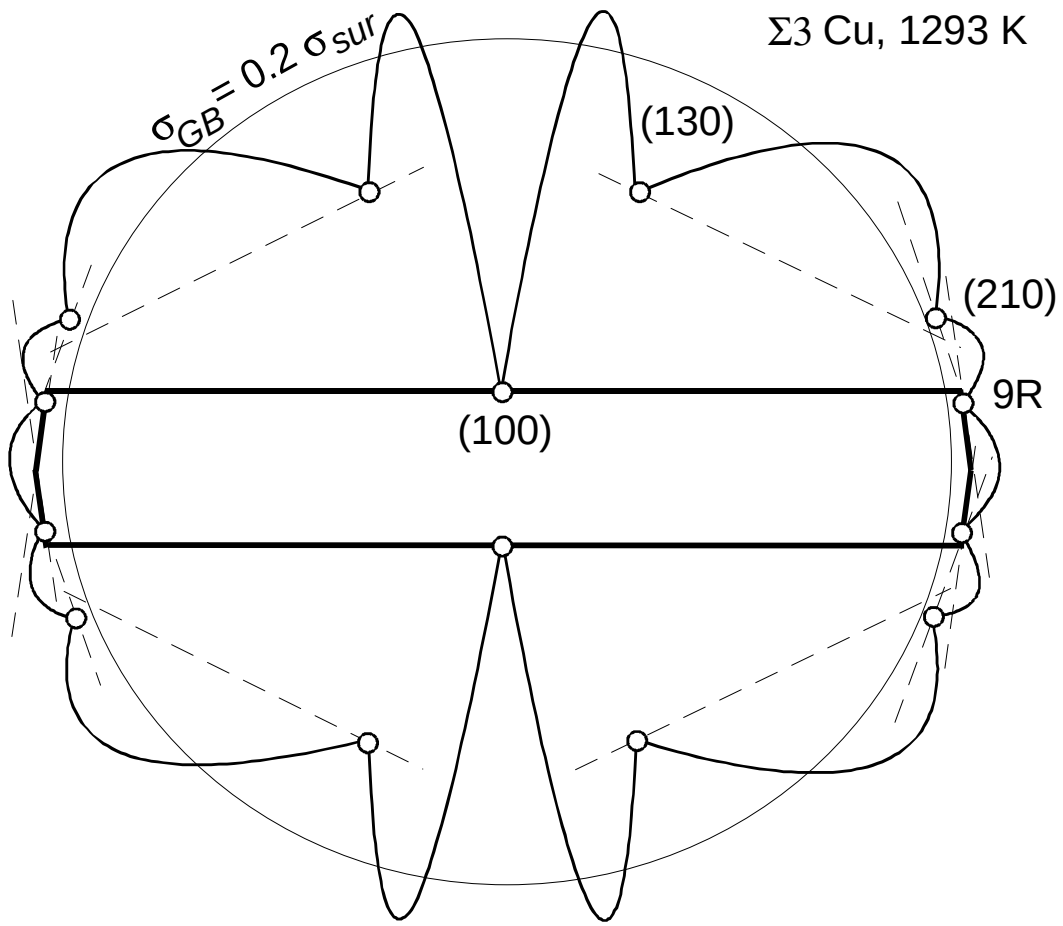

Fig. 3. Wulff-Herring plot for the Σ3 tilt [110] GBs in Cu at 1293 K. Open circles represent the GB energy σ_{GB} for various facets measured with the aid of AFM. Curved portion is hypothetical. The ring marks the value $\sigma_{GB} = 0.2\ \sigma_{sur}$.

The figure may be reduced to the one-column size

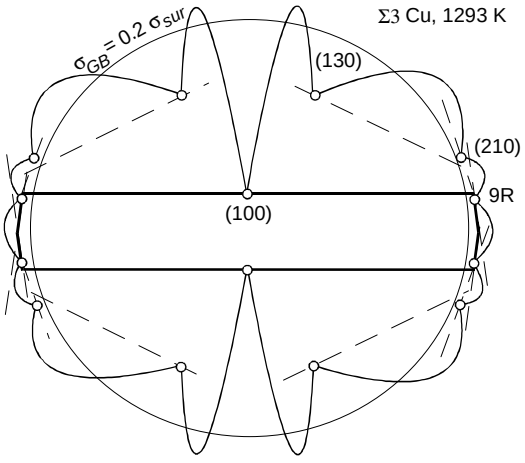

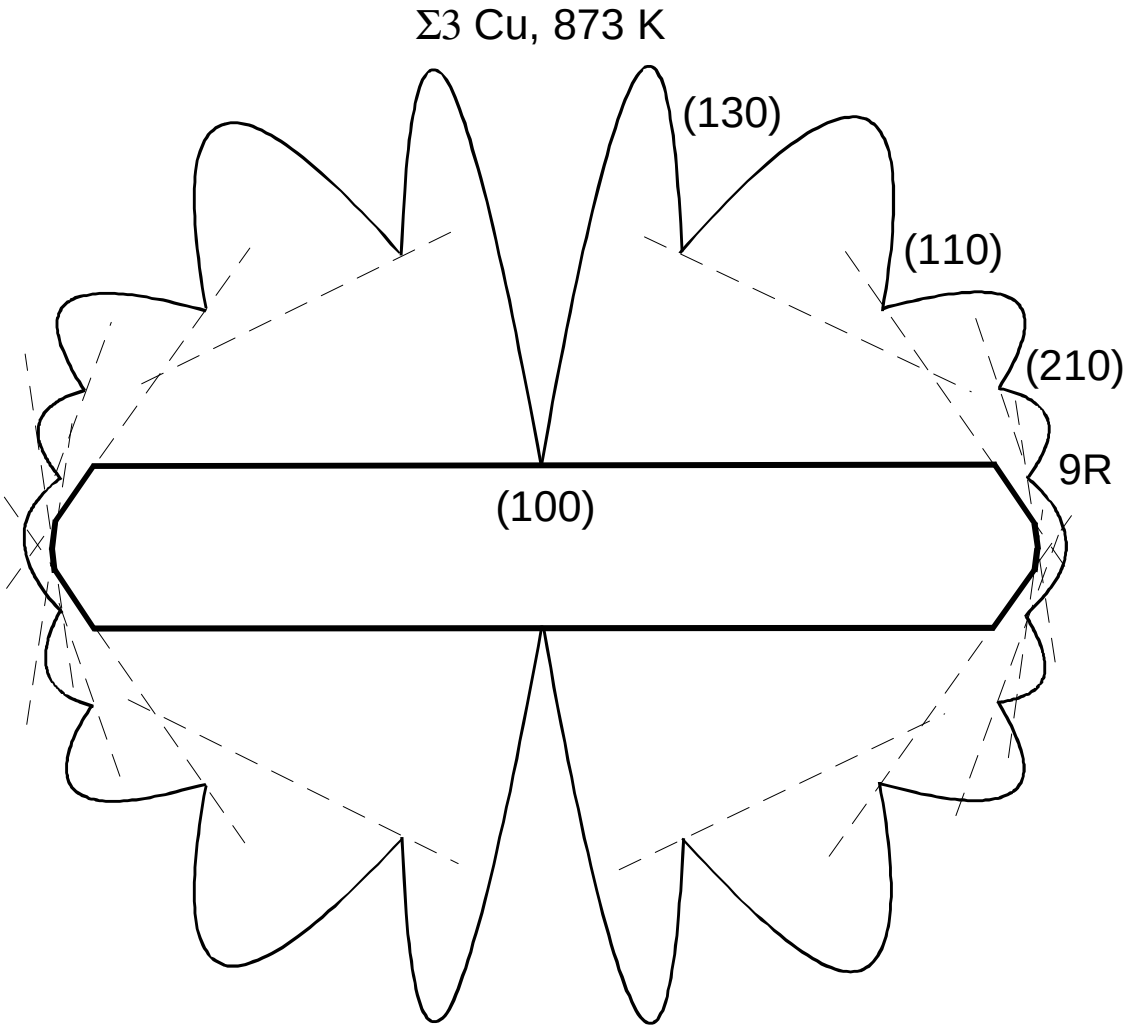

Fig. 4. Schematic Wulff-Herring plot for the Σ3 tilt [110] GBs in Cu at 873 K. Scheme is constructed using the microscopy data on presence of various GB facets after annealing.

The figure may be reduced to the one-column size

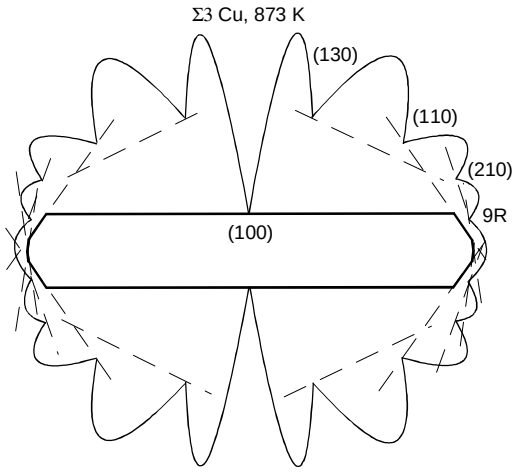

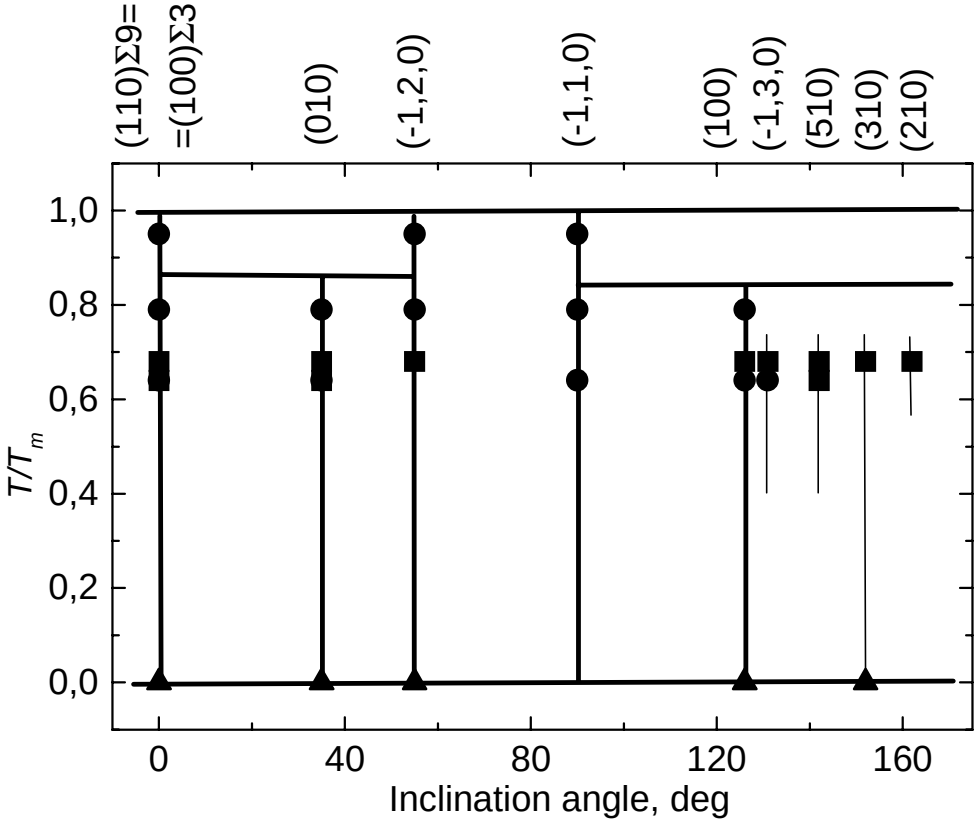

Fig. 5. Phase diagram for the various Σ9 facets. The inclinations of Σ9 CSL planes are shown at the top of the diagram. Due to the Σ9→Σ3+Σ3 dissociation, the data for $(100)_{\Sigma 3CSL}$ facet are shown instead of $(110)_{\Sigma 9CSL}$ facet. Circles denote the facets experimentally observed in this work at 0.95 T_m (1293 K), 0.79 T_m (1073 K) and 0.64 T_m (873 K). Squares denote the facets experimentally observed at 0.68 T_m [8] and at 0.64 T_m [16]. Triangles denote the energetic minima obtained using computer modelling [9]. Thick lines denote the temperature ranges of the stability for the major GB facets obtained in this work. Thin lines denote the (1) minor facet $(-1,3,0)_{CSL}$ and observed in this work and (2) the range of existence for the $(510)_{CSL}$, $(310)_{CSL}$ and $(210)_{CSL}$ facets based on the published observations of other authors [8, 16]. Horizontal lines denote the upper limits of stability for $(010)_{CSL}$ and $(100)_{CSL}$ facets.

The figure may be reduced to the one-column size

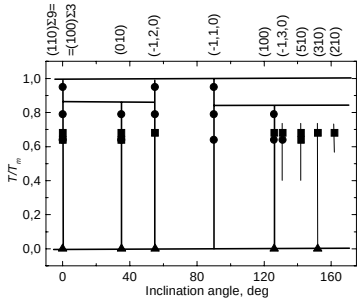

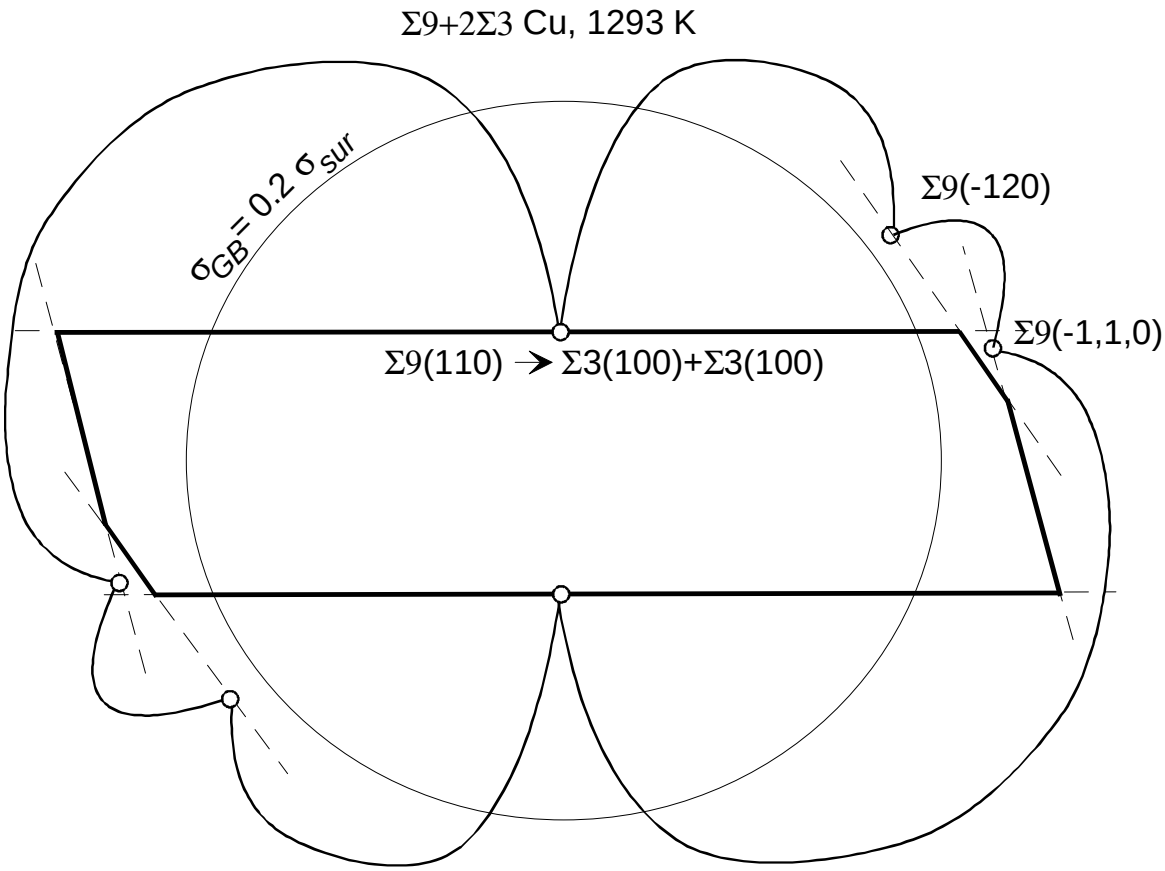

Fig. 6. Wulff-Herring plot for the Σ9 tilt [110] GBs in Cu at 1293 K. Due to the Σ9→Σ3+Σ3 dissociation, the value for two $(100)_{\Sigma 3CSL}$ facets is shown instead of $(010)_{\Sigma 9CSL}$ facet. Open circles represent the GB energy σ_{GB} for various facets measured with the aid of AFM. Curved portion is hypothetical. The ring marks the value $\sigma_{GB} = 0.2\ \sigma_{sur}$.

The figure may be reduced to the one-column size

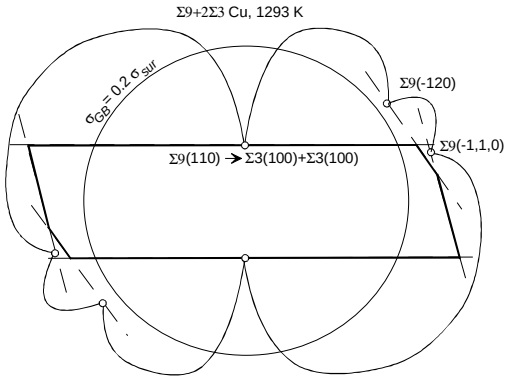

Figure captions

Fig. 1. Light micrographs showing the shape of Σ3 twin plates at (a) 1293, (b) 1073 and (c) 873 K. (a, b) Twin plates contain (100) $_{\Sigma 3CSL}$ and 82° 9*R* facets. (c) Twin plates contain (100) $_{\Sigma 3CSL}$, 82° 9*R* and 55° (110) $_{\Sigma 3CSL}$ facets.

Fig. 2. Phase diagram for the various Σ3 facets. T_m is the melting temperature. The inclinations of Σ3 CSL planes are shown at the top of the diagram. Circles denote the facets experimentally observed in this work at 0.95 T_m (1293 K), 0.79 T_m (1073 K) and 0.64 T_m (873 K). Squares denote the facets experimentally observed at 0.87 T_m [10–15, 23], at 0.64 T_m [16] and at 0.36 T_m [17]. Triangles denote the energetic minima obtained using computer modelling [19]. Thick lines denote the temperature ranges of the stability for the major GB facets obtained in this work. Thin lines denote the (1) minor facets $(120)_{CSL}$ and $(210)_{CSL}$ observed in this work and (2) the range of existence for the $(010)_{CSL}$ facet and low-temperature boundary for the 9*R* facet based on the comparison of our data with published observations of other authors [16, 17]. Horizontal lines denote the upper limits of stability for $(110)_{CSL}$ and $(010)_{CSL}$ facets.

Fig. 3. Wulff-Herring plot for the Σ3 tilt [110] GBs in Cu at 1293 K. Open circles represent the GB energy σ_{GB} for various facets measured with the aid of AFM. Curved portion is hypothetical. The ring marks the value $\sigma_{GB} = 0.2\ \sigma_{sur}$.

Fig. 4. Schematic Wulff-Herring plot for the Σ3 tilt [110] GBs in Cu at 873 K. Scheme is constructed using the microscopy data on presence of various GB facets after annealing.

Fig. 5. Phase diagram for the various Σ9 facets. The inclinations of Σ9 CSL planes are shown at the top of the diagram. Due to the Σ9→Σ3+Σ3 dissociation, the data for $(100)_{\Sigma 3CSL}$ facet are shown instead of $(010)_{\Sigma 9CSL}$ facet. Circles denote the facets experimentally observed in this work at 0.95 T_m (1293 K), 0.79 T_m (1073 K) and 0.64 T_m (873 K). Squares denote the facets experimentally observed at 0.68 T_m [8] and at 0.64 T_m [16]. Triangles denote the energetic minima obtained using computer modelling [9]. Thick lines denote the temperature ranges of the stability for the major GB facets obtained in this work. Thin lines denote the (1) minor facet $(-1,3,0)_{CSL}$ and observed in this work and (2) the range of existence for the $(510)_{CSL}$, $(310)_{CSL}$ and $(210)_{CSL}$ facets based on the published observations of other authors [8, 16].Horizontal lines denote the upper limits of stability for $(010)_{CSL}$ and $(100)_{CSL}$ facets.

Fig. 6. Wulff-Herring plot for the Σ9 tilt [110] GBs in Cu at 1293 K. Due to the Σ9→Σ3+Σ3 dissociation, the value for two $(100)_{\Sigma 3CSL}$ facets is shown instead of $(010)_{\Sigma 9CSL}$ facet. Open circles represent the GB energy σ_{GB} for various facets measured with the aid of AFM. Curved portion is hypothetical. The ring marks the value $\sigma_{GB} = 0.2\ \sigma_{sur}$.